J|A|C|S
ARTICLES
Published on Web 07/13/2002

Optical Detection of Spin Polarization in Single-Molecule Magnets $[Mn_{12}O_{12}(O_2CR)_{16}(H_2O)_4]$

Eric J. L. McInnes,[§] Elna Pidcock, Vasily S. Oganesyan, Myles R. Cheesman, Annie K. Powell,[‡] and Andrew J. Thomson*

Contribution from the School of Chemical Sciences, University of East Anglia, Norwich NR4 7TJ, U.K.

Received March 29, 2002

Abstract: A magneto-optical study has been undertaken of the mixed-valence single-molecule magnet $[Mn^{IV}_4Mn^{III}_8O_{12}L_{16}]$ in which the ligands, L, are acetate ($Mn_{12}Ac$) or the long-chain carboxylic acid, $C_{14}H_{29}$-COOH ($Mn_{12}C_{15}$), that confers better solubility in organic solvents. Thin polymer films of these compounds in poly(methyl methacrylate) (PMM) have been cast by solvent evaporation to provide samples suitable for variable-temperature and field magnetic circular dichroism (MCD) studies. The absorption spectra in isotropic light are featureless, whereas the low-temperature MCD spectra contain resolved peaks, both positive and negative. MCD magnetization curves measured at temperatures above 4.2 K have established a ground-state spin of $S = 10$ and an axial zero-field parameter, D, of -0.61 K, similar to that determined for single crystals of $Mn_{12}Ac$. By studying at a variety of optical wavelengths, the polarization ratios of the optical transitions relative to the unique axis of the zero-field distortion have been determined. The MCD magnetization curves measured at 4.2 K between 0 and 5 T for the case of $Mn_{12}C_{15}$ in the PMM film can be fitted only on the assumption of nonrandom distribution of molecular *z*-axes arising from stresses in the polymer film during the process of casting. MCD-detected hysteresis curves measured in both frozen solution and PMM films, below the blocking temperature of $\sim$3 K, show a high retention of spin polarization after reduction to zero of a polarizing magnetic field. This generates intense zero-field circular dichroism (CD) with maximum intensity for *xy*-polarized optical transitions whose sign depends on the direction of the original polarizing field. The optical polarization and the selection rules for MCD select a subset of molecular orientations with respect to the direction of field. Thus, the magnetically induced CD provides a highly sensitive and rapid optical method of reading the spin polarization of molecular magnets.

Introduction

The need for small magnetic particles capable of storing data at high densities is driving research into the synthesis and understanding of single-molecule magnets (SMMs). An SMM is a compound that displays hysteresis in its magnetic susceptibility vs external field loop, which is of a *molecular* origin.[1] One of the most widely studied SMMs to date is the mixed-valence manganese cluster $[Mn_{12}O_{12}(O_2CR)_{16}(H_2O)_4]$.[2] It comprises four Mn(IV) ions ($S = 2$) in a $Mn^{IV}_4O_4$ cubane-like core surrounded by eight outer Mn(III) ions ($S = {}^3/_2$) bridged by carboxylate oxygen atoms (Chart 1). Exchange interactions within the cluster result in an overall ground-state spin of $S = 10$.[3,4] However, the cluster framework of Mn ions is axial to a high level of approximation with the unique *z*-axis along the S_4 axis of the $Mn^{IV}O_4$ cubane core. This distortion induces a zero-field splitting (ZFS), defined as D in the spin Hamiltonian, which has been determined to be negative, ~ -0.5 cm^{-1}.[5,6] Hence, the 21 M_s sublevels of the $S = 10$ ground state are split, in zero magnetic field, into $M_s = \pm n$ sublevels (where $n = 0-10$), with

Chart 1. Structure of $Mn_{12}O_{12}$ Core of $[Mn_{12}O_{12}(O_2CMe)_{16}(H_2O)_4]$ with Ligand Framework Removed[a]

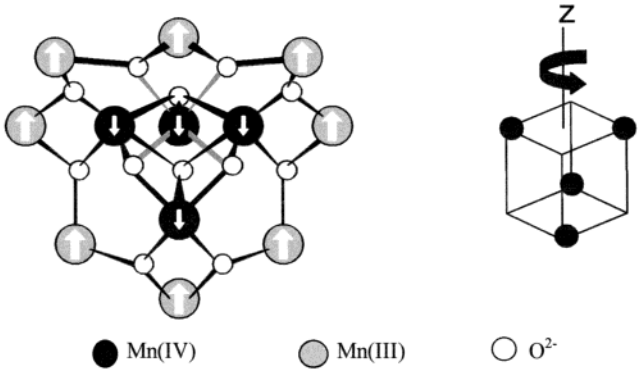

[a] Arrows denote relative directions of electron spins in the lowest M_s state. The direction of the unique S_4 axis relative to the $Mn^{IV}O_4$ cube is shown.

* To whom correspondence should be addressed. E-mail: a.thomson@uea.ac.uk. Phone: +44 1603 592005. Fax: +44 1602 592003.
[§] Present address: Department of Chemistry, University of Manchester, Oxford Road, Manchester M13 9PL, UK.
[‡] Present address: Institut für Anorganische Chemie, Universität Karlsruhe, Engesserstrasse Geb. 30.45, D-76128 Karlsruhe, Germany.

(1) For example, see: Aubin, S. M. J.; Sun, Z.; Pardi, L.; Krzystek, J.; Folting, K.; Brunel, L.-C.; Rheingold, A. L.; Christou, G.; Hendrickson, D. N. *Inorg. Chem.* **1999**, *38*, 5329 and references therein.
(2) Lis, T. *Acta Crystallogr.* **1980**, *B36*, 2042.

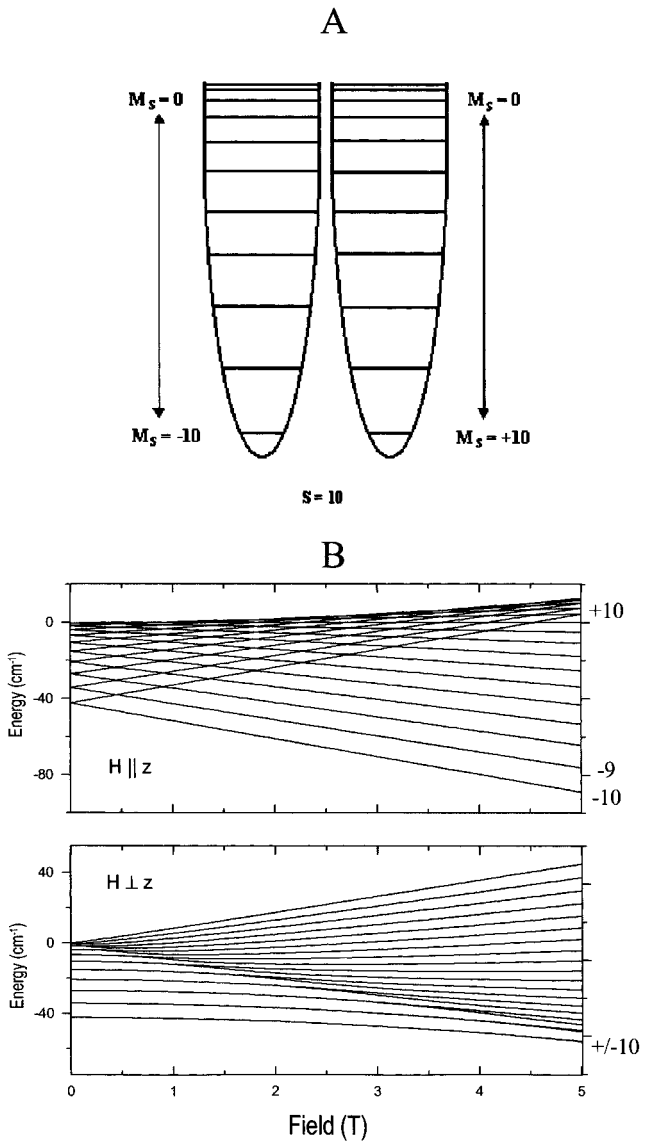

Figure 1. Electronic energy levels of the $Mn_{12}O_{12}$ core of $[Mn_{12}O_{12}(O_2CMe)_{16}(H_2O)_4]$. **(A)** Ground-state spin states, $S = 10$, subject to an axial zero-field splitting of $-D \cdot S_z^2$ in zero magnetic field and **(B)** as a function of applied magnetic fields parallel and perpendicular to *z*.

the $M_s = \pm 10$ pair lying lowest in energy, approximately 50 cm^{-1} (given by $D \cdot S_z^2$) below the single $M_s = 0$ sublevel (Figure 1A). This manifold of spin sublevels provides an energy barrier to interconversion of up and down electron spins between, for instance, $M_s = +10$ and -10 levels. Thermally activated relaxation of spins over this barrier, governed by the Arrhenius law, is fast at high temperatures. Conversely, at very low temperatures, below 3 K,[4] spin relaxation becomes very slow. Hence, spin populations can be effectively trapped in the lowest energy sublevel. Application of a magnetic field parallel to the *z*-axis creates spin polarization by removing the degeneracy of the $M_s = \pm n$ sublevels and preferentially populating the lower energy sublevels (Figure 1B). Below 3 K, the so-called "blocking temperature", spin polarization remains trapped, even after removal of the magnetic field, leading to magnetic hysteresis. Relaxation of spin polarization can occur below the blocking temperature via mechanisms other than thermal activation, such as quantum tunneling of magnetization between quasi-degenerate sublevels.[7−9] Evidence for this phenomenon has been observed for Mn_{12} as distinct steps in measurements of susceptibility vs magnetic field on oriented samples when the field is applied parallel to the unique axis of the molecule.[7−9] Application of a magnetic field perpendicular to the unique *z*-axis causes a mixing of M_s sublevels that differ by ± 1 (Figure 1B). Hence, a nonzero component of an applied field perpendicular to *z* provides, in high order, a path for relaxation between the up and down spin manifolds.

It is this group of phenomena that has created so much interest in this class of SMMs. For example, information could be stored as up or down spins, and the information would remain as long as the spin polarization persists. A magnetic field provides a method of inducing or erasing electron spin polarization and hence information. Recently, interest has grown in the use of optical methods of reading the sign and extent of spin polarization and, possibly, of creating or erasing spin polarization in SMMs. Optical methods provide a highly sensitive and rapid way to read such information. To date, the orientation-dependent, ground-state properties of the Mn_{12} cluster have been probed through bulk measurements such as susceptibility using single crystals or oriented crystallites. These states of the material are not convenient for optical studies. In this paper we present data on Mn_{12} clusters obtained using magnetic circular dichroism (MCD) spectroscopy on frozen solutions and in polymer films in order to investigate the feasibility of optical readout and control. We show that MCD is a powerful tool in the study of these molecular nanomagnets. The single-ion electronic transitions are rather well resolved in the MCD spectrum, whereas they are poorly resolved in the absorption spectrum measured with unpolarized light. The intensity and sign of absorption of circularly polarized photons measure the spin polarization of the ground state induced by the application of a magnetic field. Furthermore, because of the axial distortion, the optical transitions can be strongly polarized either parallel or perpendicular to the unique axis, that is, *z* or *xy*. The selection rules for absorption of circularly polarized photons ensure that, for each optical transition, only a subset of molecules are excited, depending on the polarization direction and orientation with respect to the applied magnetic field. Thus, information which is wavelength, and hence orientation, dependent can be obtained from isotropic samples.

We have previously reported the MCD spectra of $[Mn_{12}O_{12}(O_2CMe)_{16}(H_2O)_4]$ in dmf/MeCN (dmf = *N*,*N*-dimethylformamide) solution at 4.2 and 1.7 K.[10] Although the absorption spectrum at room temperature was devoid of resolved features in the 400−850 nm wavelength range, the MCD spectrum at 4.2 K revealed a series of broad positive and negative bands. Moreover, we found that after application of a magnetic field (±5 T) to a sample at 1.7 K, a strong circular dichroism (CD)

(3) Sessoli, R.; Tsai, H.-L.; Schake, A. R.; Wang, S.; Vincent, J. B.; Folting, K.; Gatteschi, D.; Christou, G.; Hendrickson, D. N. *J. Am. Chem. Soc.* **1993**, *115*, 1804−1816.
(4) Sessoli, R.; Gatteschi, D.; Caneschi, A.; Novak, M. A. *Nature* **1993**, *365*, 141−143.
(5) Barra, A.-L.; Gatteschi, D.; Sessoli, R. *Phys. Rev. B* **1997**, *56*, 8192−8198.
(6) Hill, S.; Perenboom, J. A. A. J.; Dalal, N. S.; Hathaway, T.; Stalcup, T.; Brooks, J. S. *Phys. Rev. Lett.* **1998**, *80*, 2453.
(7) Chudnovsky, E. M. *Science* **1996**, *274*, 938−939.
(8) Thomas, L.; Lionti, F.; Ballou, R.; Gatteschi, D.; Sessoli, R.; Barbara, B. *Nature* **1996**, *383*, 145−147.
(9) Friedman, J. R.; Sarachik, M. P.; Tejada, J.; Ziolo, R. *Phys. Rev. Lett.* **1996**, *76*, 3830−3833.
(10) Cheesman, M. R.; Oganesyan, V. S.; Sessoli, R.; Gatteschi, D.; Thomson, A. J. *Chem. Commun.* **1997**, 1677−1678.

spectrum remained at zero magnetic field. This spectrum was essentially identical to that recorded at ±5 T, but with only ca. 30% of the original intensity. The sign of the residual spectrum depended on the direction of the original magnetic field (+ or −), and hence the CD signal at zero field reported the magnetic history of the sample, giving rise to a form of optical bistability. Here we report new MCD studies on $[Mn_{12}O_{12}(O_2CR)_{16}(H_2O)_4]$ (R = Me, *n*-$C_{14}H_{29}$) in frozen organic glasses and plastic films. Derivatization of the ligands allows good optical quality polymer films of these materials to be cast. We demonstrate that the hysteresis effects are wavelength dependent, correlating with the polarizations of the optical transitions.

Experimental Section

Synthesis. Christou et al. have prepared a number of derivatives of $[Mn_{12}O_{12}(O_2CMe)_{16}(H_2O)_4]$ by simple substitution reactions with RCO_2H.[3,11] We have followed similar synthetic procedures.

(i) $[Mn_{12}O_{12}(O_2CMe)_{16}(H_2O)_4]\cdot MeCO_2H\cdot 4H_2O$ ($Mn_{12}Ac$). The method of Lis,[2] as modified by Eppley et al.,[11] was used for preparation.

(ii) $[Mn_{12}O_{12}(O_2CR)_{16}(H_2O)_4]$ (R = *n*-$C_{14}H_{29}$) ($Mn_{12}C_{15}$). A suspension of $C_{14}H_{29}CO_2H$ (2.5 g, 10.3 mmol) and $Mn_{12}Ac$ (0.5 g, 0.24 mmol) in Et_2O (50 mL) was stirred at room temperature for 4 h to give a dark brown solution. The volume of solvent was reduced in vacuo to a few milliliters. Toluene (10 mL) was added and the solution concentrated in order to remove free acetic acid.[11] A further two portions of toluene (10 mL) were added and removed in vacuo. The resultant solid was stirred in acetone (100 mL), whereupon excess ligand dissolved to leave a brown solid which was separated by filtration, washed with copious acetone, and air-dried. The isolated waxy brown product was suspended in Et_2O (50 mL) with $C_{14}H_{29}CO_2H$ (2.0 g, 8.3 mmol) and the entire procedure repeated until the final product gave a satisfactory elemental analysis (three or four repetitions). Elemental analysis, C:H 59.7:9.86 (calculated for $C_{240}H_{468}O_{48}Mn_{12}$, 60.2:9.96). Selected IR data (KBr): 3325 (br), 2920 (s), 2853 (s), 1586 (s), 1500 (s), 1420 (s), 1100 (s), 1023 (s), 804 (s), 724 (s), 645 (s), 612 (sh), 545 (m), 520 (m).

Although the long aliphatic tails of the ligands in $Mn_{12}C_{15}$ prevent crystallization of the compound, the integrity of the $[Mn_{12}O_{12}]$ core is confirmed by the characteristic Mn−O stretches in the IR spectra (given by Eppley et al.)[11] and also by the distinctive magnetic and MCD behavior (see later). $Mn_{12}Ac$ is soluble only in reasonably polar, coordinating solvents such as MeCN. $Mn_{12}C_{15}$ has much improved solubility, even dissolving in highly nonpolar, noncoordinating solvents such as Et_2O or hexane. This allows the formation of plastic (PMM) films which are convenient for low-temperature spectroscopic studies. Mixed solvents were required to dissolve the polymer ($CHCl_3$) and complex (MeCN) in the case of $Mn_{12}Ac$, and this tends to result in lower concentrations of solute and thinner films.

(iii) Poly(methyl methacrylate) (PMM) Films of $Mn_{12}C_{15}$. PMM (200 mg, approximately M_w 996 000) and $Mn_{12}C_{15}$ (7 mg) were dissolved in $CHCl_3$ and filtered, and a few drops of the solution were dropped on a glass slide. The slide was protected from dust by covering with an overturned watchglass, and the solvent was allowed to evaporate slowly overnight. The resulting brown, transparent thin films were easily removed from the slide with a razor blade.

(iv) PMM Film of $Mn_{12}Ac$. PMM (200 mg) and $Mn_{12}Ac$ (9 mg) were dissolved in MeCN/$CHCl_3$ (4 mL, 1:1 v/v) and treated as above. The films were separated from the slide by bathing in warm water for a few minutes and were dried on filter paper.

MCD Spectroscopy. MCD measurements were performed as reported elsewhere.[12]

Analysis of MCD Magnetization Curves. To calculate MCD magnetization curves and the temperature dependences of MCD intensities for optical transitions with different polarizations, the following spin Hamiltonian has been employed:

$$\hat{H} = D(S_z^2 - S^2/3) + g\beta\vec{S}\vec{H} \tag{1}$$

Although higher order terms $B_4^0O_4^0 + B_4^4O_4^4$ in the spin Hamiltonian appear to be crucial for relaxation phenomena via tunneling below the blocking temperatures,[5] they are of the order of $|B_4^0| = 2.2 \times 10^{-5}$ cm^{-1}, $|B_4^4| = 4 \times 10^{-5}$ cm^{-1}, and hence too small to be significant for MCD magnetization curves. This was confirmed by simulations of magnetization curves using a spin Hamiltonian with and without these additional terms. The curves are indistinguishable. MCD magnetization curves and temperature dependences were calculated on the basis of theoretical approaches developed for the analysis of high-spin metal ions.[13a−c] These approaches are also applicable to oligomeric transition metal species coupled by exchange interactions. For a particular transition, the MCD intensity consists of temperature-dependent and temperature-independent terms. The former is due to spin−orbit coupling between the ground and excited states or within excited states, while the orbital angular momentum component of the Zeeman interaction is responsible for the appearance of temperature-independent terms. The latter are usually negligible compared with temperature-dependent contributions, especially at very low temperature. Within each monomer, transitions to an orbitally nondegenerate excited state show MCD with Gaussian bands shapes and temperature-dependent terms according to the following relationship:

$$\Delta\epsilon(T,H,\nu) = Kf(\nu,\nu_0,\Delta)(\langle S_z\rangle_T\tilde{M}_x\tilde{M}_y + \langle S_x\rangle_T\tilde{M}_x\tilde{M}_z + \langle S_y\rangle_T\tilde{M}_y\tilde{M}_z) \tag{2a}$$

In the case of tetragonal symmetry, this reduces to the following form:

$$\Delta\epsilon(T,H,\nu) = Kf(\nu,\nu_0,\Delta)(\langle S_z\rangle_T\tilde{M}_x\tilde{M}_y + \langle S_\perp\rangle_T\tilde{M}_\perp\tilde{M}_z) \tag{2b}$$

$\langle S_z\rangle$ and $\langle S_\perp\rangle$ are projections, parallel and perpendicular to the easy axis, respectively, of the net expectation value of the spin of the ground state induced by the magnetic field. In the case of molecules in frozen solution, these expressions are thermally and orientationally averaged as follows:

$$\langle S_z\rangle_T = \frac{1}{2}\int_0^\pi \sum_g \langle S_z\rangle_{gg} \frac{\exp(-E_g/kT)}{\sum_g \exp(-E_g/kT)} \cos\vartheta \sin\vartheta \, d\vartheta$$
$$\langle S_\perp\rangle_T = \frac{1}{2}\int_0^\pi \sum_g \langle S_x\rangle_{gg} \frac{\exp(-E_g/kT)}{\sum_g \exp(-E_g/kT)} \sin^2\vartheta \, d\vartheta \tag{3}$$

$\langle S_k\rangle_{gg}$ is the net expectation value of the operator S_k when the system is in a state g, and $f(\nu,\nu_0,\Delta)$ is a Gaussian band shape function, where Δ is the bandwidth. $\tilde{M}_i\tilde{M}_j$ is the product of two perpendicular components of transition dipole moments, one being induced by spin−orbit coupling with other states. Both components lie in a plane perpendicular to the appropriate component of the induced spin momentum of the ground manifold. These products measure circular polarization in the plane.

For clusters of paramagnetic ions coupled by an exchange interaction, J, in the case that $J \gg \Delta$ and $J \gg kT$, eq 2 is applicable to the whole system, with $\langle\vec{S}\rangle$ being the net expectation value of the overall spin of the cluster. The polarization products $\tilde{M}_i\tilde{M}_j$ for single-ion optical transitions need to be calculated in the same coordinate system as $\langle\vec{S}\rangle$. Subsequent analyses present all quantities in the molecular cluster symmetry coordinate system. The collection of constants, K, in eq 2 is a complex function of single spins of coupled ions, $K(S_1,S_2,...,S_{12})$, that

(11) Eppley, H. J.; Tsai, H.-L.; de Vries, N.; Folting, K.; Christou, G.; Hendrickson, D. N. *J. Am. Chem. Soc*. **1995**, *117*, 301−317.
(12) Thomson, A. J.; Cheesman, M. R.; George S. J. *Methods Enzymol*. **1993**, *226*, 199−232.

depends on the way these spins are coupled to each other through $3-j$, $6-j$, and $9-j$ coefficients. We note that, in the case of weak exchange-coupled ions, when $J \ll \Delta$ and/or $J \ll kT$, the modified equation is no longer valid.[13d] In this case, for each transition only the contribution from a single ion to the net expectation value of $\langle S_k \rangle_T$ is needed. Generally, and especially for a low-symmetry system, this could lead to the situation where transitions of the same polarization but localized at different centers would possess different magnetization curves.

A computer program for the simulation of MCD magnetization curves developed previously[13a,e] has been adapted for the simulation and fitting of curves measured at different wavelengths. In this program, the spin Hamiltonian is diagonalized, and the resulting energies and wave functions are used for calculation of $\langle S_k \rangle_T$. Fitting experimental curves by use of eqs 1−3 permits the determination of the ZFS parameter D as well as the relative contributions from different polarization products at each particular wavelength.

Within the low-temperature limit ($T \leq 4.2$ K), only the lowest non-Kramers doublet $M_s = \pm 10$ is populated and, given that $g\beta H \sin \vartheta \ll 19|D|$, perturbation theory for degenerate states is applicable. The parallel component of the applied magnetic field will split these states, while the component in the xy plane mixes them with states $M_s = \pm 9$ to first order. $M_s = \pm 9$ are the only spin states allowed to mix with the lowest doublet by the selection rules for matrix elements of the Zeeman interaction. Under these conditions, the linear field approximation is valid and the behavior of magnetization curves can be rationalized in terms of the well-known C and B terms formalism.[13f,g] Using these approximations, one can reduce eq 3 to the following simple form:

$$\Delta\epsilon(T,H,\nu) = Kf(\nu,\nu_0,\Delta)\left(\tilde{M}_x\tilde{M}_y \frac{5}{2}\int_0^{\pi} \tanh\left(\frac{g_{\parallel}\beta H \cos\vartheta}{2kT}\right)\sin 2\vartheta \, d\vartheta + \tilde{M}_{\perp}\tilde{M}_z H \frac{2\sqrt{5}}{3}\frac{g\beta}{19D}\right) \quad (4)$$

This equation shows that the contributions to the MCD spectra from xy-polarized transitions is temperature dependent (C term). Hence, the intensity of the MCD depends on the population of the lowest spin states and as a result is sensitive to relaxation mechanisms. On the other hand, MCD terms due to transitions polarized in xz or yz planes originate from Zeeman interactions between the lowest spin states, $M_s = \pm 10$, and excited states and is therefore temperature independent (B term). This term is linear in field and does not contribute to the retention of magnetization below the blocking temperatures. Note that the term B is temperature independent only at low temperatures, $kT \ll 19|D|$), where spin states with $|M_s| < 10$ remain unpopulated. When $M_s = \pm 9$ states have substantial population, they will compensate for the contribution from $M_s = \pm 10$ states because of the opposite sign of the denominator in the second term of the right side of eq 4, thus reducing the overall contribution of the B term to the MCD intensity.[13f,g] This is distinct from the temperature-independent effects arising from the orbital angular momentum components of the Zeeman interaction (see earlier).

Results and Discussion

Absorption and MCD Spectra. (i) $Mn_{12}C_{15}$. The room-temperature electronic absorption spectrum of $Mn_{12}C_{15}$ in the polymer film PMM is shown in Figure 2A. The spectrum of a frozen solution of $Mn_{12}C_{15}$ in $CHCl_3$/toluene (1:1 v/v) is broadly similar to that of the film and is devoid of resolved features (not shown). MCD spectra, at 5 T and 1.8 K, were obtained of $Mn_{12}C_{15}$ in $CHCl_3$/toluene (50/50 v/v) and a PMM film (Figure 2B,C). The spectra have clearly resolved MCD peaks at ca. 28 000 (positive sign in positive magnetic field), 26 000 (positive, shoulder), 23 500 (negative), 21 200 (negative), 19 600 (negative), 18 000 (negative), and 16 000 cm^{-1} (positive). The CD spectra were measured after the magnetic field had been ramped to zero (Figure 2B,C). A high degree of dichroism persists, the intensity of which is clearly wavelength dependent.

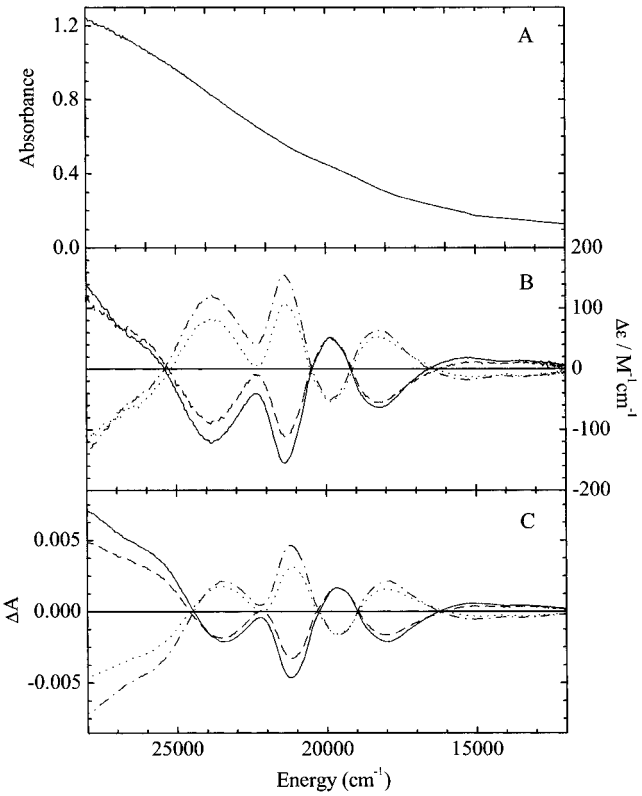

Figure 2. **(**A**)** Electronic absorption spectrum of $Mn_{12}C_{15}$ in PMM polymer film at room temperature. **(B)** MCD spectra of $Mn_{12}C_{15}$ in $CHCl_3$/toluene (50:50 v/v) measured at 1.8 K: (—) +5 T, (— • —) −5 T, and (- - -) 0 T after application of +5 T field and (•••) after application of −5 T field. **(C)** MCD spectra of $Mn_{12}C_{15}$ in PMM film measured at 1.8 K: (—) +5 T; (— • —) −5 T, and (- - -) 0 T after application of +5 T field and (•••) after application of −5 T field.

(ii) $Mn_{12}Ac$. The absorption spectra of $Mn_{12}Ac$ in solutions of MeCN/dmf (3:1 v/v) and PMM films (data not shown) were also devoid of resolved features but were similar to each other and to those obtained for $Mn_{12}C_{15}$. MCD spectra obtained at 1.7 K and 5 T of the film and a frozen solution in dmf/MeCN are shown in Figure 3. The spectra resemble those of $Mn_{12}C_{15}$, indicating that the aliphatic chains of the $Mn_{12}C_{15}$ ligand do not perturb the $Mn_{12}O_{12}$ core. The solution and film spectra reveal slight differences from those of $Mn_{12}C_{15}$, particularly in the ratios of the band intensities and in the region of 19 000−25 000 cm^{-1}; for example, the solution spectra show little positive intensity at 19 500 cm^{-1}. Below 2 K, the retention of spin polarization as judged by the zero-field CD spectrum varies both with nature of the sample and with wavelength. The MCD spectra at 4.2 K and 5 T (not shown) are broadly similar for both $Mn_{12}C_{15}$ and $Mn_{12}Ac$.

(13) (a) Oganesyan, V. S.; George, S. J.; Cheesman, M. R.; Thomson, A. J. *J. Chem. Phys.* **1999**, 110, 762−777. (b) Oganesyan, V. S.; Thomson, A. J. *J. Chem. Phys.* **2000**, 113, 5003−5017. (c) Neese, F.; Solomon E. I. *Inorg. Chem.* **1999**, *38*, 1847−1865. (d) Oganesyan, V. S.; Thomson, A. J., unpublished results. (e) Oganesyan, V. S.; Sharonov, Y. A. *Spectrochim. Acta* **1997**, *53A*, 433−449. (f) Stephens, P. J. *Adv. Chem. Phys.* **1976**, *35*, 197−264. (g) Piepho, S. B.; Schatz, P. N. *Group Theory in Spectroscopy with Applications to Magnetic Circular Dichroism*; Wiley & Sons: New York, 1983. (h) Hunter, D. J. B.; Oganesyan, V. S.; Salerno, J. C.; Butler, C. S.; Ingledew, W. J.; Thomson, A. J. *Biophys. J.* **2000**, *78*, 439−450.

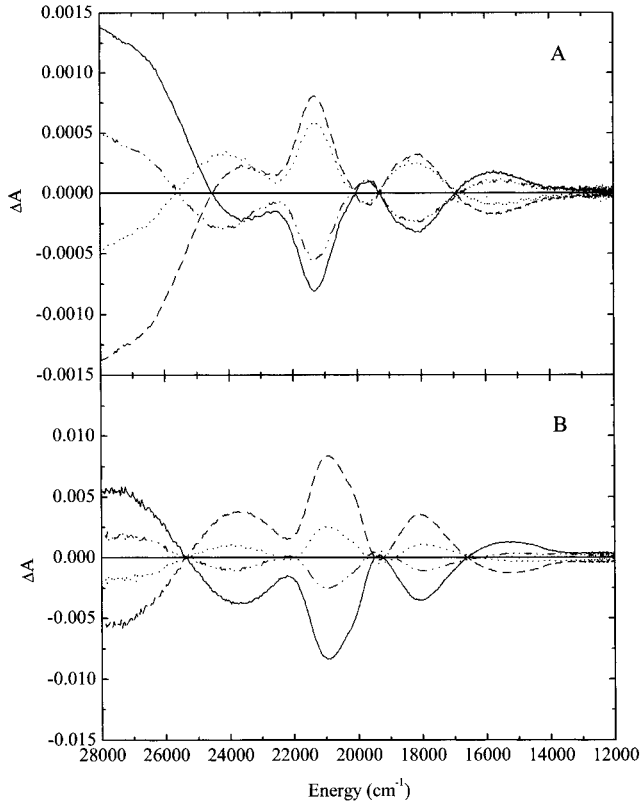

Figure 3. MCD spectra of $Mn_{12}Ac$ recorded at 1.7 K **(A)** in PMM film and **(B)** in dmf/MeCN (3:1 v/v) solution: (—) +5 T, (– ·· –) 0 T after application of +5 T, (– – –) −5 T, and (···) 0 T after application of −5 T.

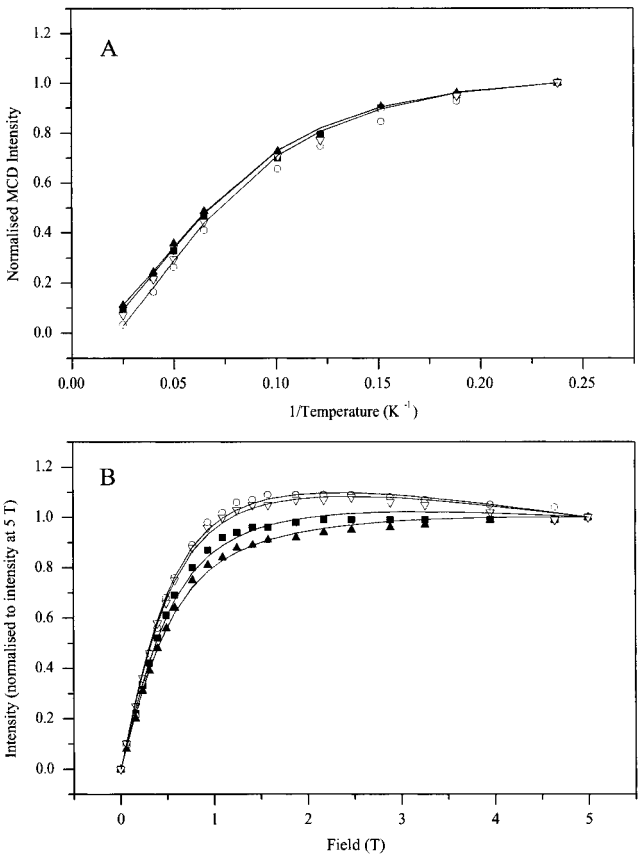

Figure 4. **(A)** Normalized MCD intensity versus temperature (K) for transitions of $Mn_{12}C_{15}$ in PMM film at a constant field of 1 T: (■) 18 000, (○) 19 600, (▲) 21 200, and (▽) 23 400 cm^{-1}. Temperatures between 4.2 and 40 K; (—) fit to spin $S = 10$ and $D = -0.6$ K. **(B)** MCD magnetization curves measured at 4.2 K between 0 and 5 T for transitions of $Mn_{12}C_{15}$ in PMM film: (■) 18 000, (○) 19 600, (▲) 21 200, and (▽) 23 400 cm^{-1}; (—) simulations with parameters $S = 10$, $D = -0.6$ K, $\vartheta = 90°$, $\sigma \approx 35°$, and polarization ratios given in Table 1.

MCD Magnetization Properties above the Blocking Temperature. Above the blocking temperature, spin relaxation is rapid, and hence hysteretic effects will be absent. Thus, in this temperature regime, the MCD spectra can be used to determine zero-field parameters of the ground state and the polarization ratios of the optical transitions.

At 4.2 K, the MCD spectra of $Mn_{12}Ac$ and $Mn_{12}C_{15}$ at +5 and −5 T are equal in intensity but differ only in the signs of the transitions. After lowering the field to zero with the sample held at 4.2 K, the CD intensity is zero at all wavelengths. The value of *D*, the axial distortion parameter, has been determined by measuring the temperature dependence, between 4.2 and 40 K, of the MCD intensity of $Mn_{12}C_{15}$ at a field of 1 T (Figure 4A). The magnetic field strength of 1 T was chosen to ensure that Zeeman effects are small compared with *kT* so that the results are independent of optical polarization. Data were collected for optical transitions at 18 000, 19 600, 21 200, and 23 400 cm^{-1}. A good fit was obtained for *D* of −0.6 K, a value very similar to the *D* value measured for $Mn_{12}Ac$ using high-frequency EPR,[14] showing that the ground-state magnetic properties of $Mn_{12}C_{15}$ are similar to those of $Mn_{12}Ac$.

To determine the polarization ratios of the optical transitions, magnetization curves of $Mn_{12}Ac$ were collected at 4.2 K between fields of 0 and 5 T in frozen solution at 21 050 and 18 020 cm^{-1} (Figure 5). The lowest Kramers doublet with $M_s = \pm 10$ has effective *g* values of $g_{\|} = 40$ and $g_{\perp} = 0$. Therefore, magnetic saturation can be reached even at 4.2 K and fields up to 5 T. Curves were simulated using the reported values for *D* of −0.61 K and *E* of 0.[8] The polarization ratio of the various optical transitions is the only variable. Good agreement was obtained between calculated and experimental curves (Figure 5). The transition at 18 200 cm^{-1} is *xy*-polarized, whereas that at 21 000 cm^{-1} corresponds to an equal mixture of *xy* and *xz*/*yz* polarizations; that is, the transition is essentially isotropic. The contributions from a purely *xy*-polarized transition are shown by a dotted line, while those in *xz* or *yz* planes are represented by a dashed line (Figure 5).

Attempts to fit MCD magnetization curves of $Mn_{12}C_{15}$ measured in PMM films using similar procedures were unsatisfactory at all wavelengths tested. Although the shape of the magnetization curves close to the saturation limit can be reproduced well, simulations fail to reproduce the initial slopes of the experimental curves below fields of 1 T. The fits failed to improve, even when tested for ground-state spins different from $S = 10$. Inclusion of a Zeeman interaction between the ground spin manifold and other, higher lying multiplets also fails to improve the fit, resulting only in an additional *B* term contribution to eq 4 which is linearly dependent on field. Therefore, we have investigated the possible effects of an anisotropic distribution of $Mn_{12}C_{15}$ molecules within the film of PMM. This can be modeled by averaging the probability of the orientation of the unique axis away from random distribution.

(14) Caneschi, A.; Gatteschi, D.; Sessoli, R.; Barra, A. L.; Brunel, L. C.; Guillot, M. *J. Am. Chem. Soc.* **1991**, *113*, 5873.

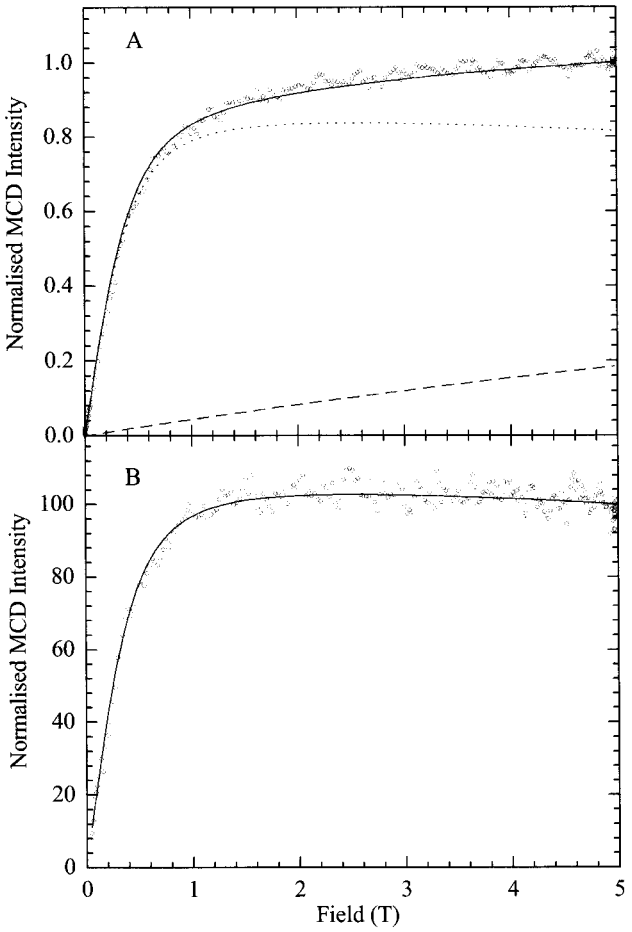

Figure 5. MCD magnetization curves of $Mn_{12}Ac_{12}$ in dmf/MeCN (3:1 v/v) measured between 0 and 5 T at 4.2 K at wavelengths of **(**A**)** 475 nm and **(**B**)** 550 nm (○): (—) fit to data points with polarization ratios from Table 1; theoretical curves for (···) pure *xy* and (---) *zx* (*zy*)-polarized transitions.

This allows an angular spread, σ, about a fixed angle ϑ_0. A Gaussian distribution of the symmetry axis, *z*, of the $Mn_{12}C_{15}$ cluster relative to the magnetic field direction, applied normal to the plane of the film, is given by

$$Q(\vartheta - \vartheta_0) = \exp\left(-\left(\frac{\vartheta - \vartheta_0}{\sigma}\right)^2\right)$$

where ϑ_0 is the mean value of the angle between *z* and the magnetic field, and σ is the half-width of the cone of angular spread. Averaging is performed by numerical integration followed by division with a normalizing factor

$$N(\vartheta_0,\sigma) = 2\pi\int_0^{\pi} Q(\vartheta - \vartheta_0)\sin\vartheta\,\mathrm{d}\vartheta$$

which depends on both ϑ_0 and σ. For isotropic distribution around the unit sphere, as for molecules in frozen solution, we let $\sigma \rightarrow \infty$ when $N(\vartheta_0,\sigma)$ reduces to 4π. For partially oriented molecules, our model assumes a uniform distribution in the plane of polymer film and partial orientation in planes containing the normal to it. The detailed calculations of the MCD of anisotropically distributed, paramagnetic molecules will be published elsewhere, but the treatment follows the approach adopted for analysis of the EPR spectra of partially oriented membranes of protein.[13h]

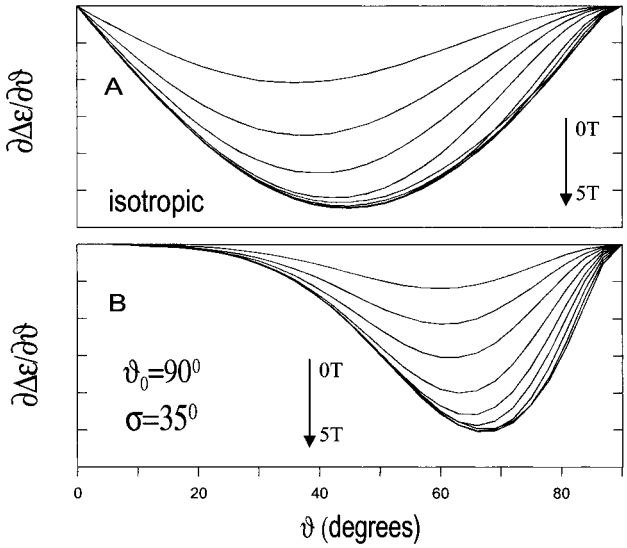

Figure 6. Calculated MCD intensities of an *xy*-polarized transition **(**A**)** for molecules of $Mn_{12}O_{12}$ with *z*-axes randomly distributed at angles between $\vartheta = 90°$ and $\vartheta = 0°$ and **(**B**)** a set of molecules with an anisotropic distribution of *z*-axes about an angle $\vartheta_0 = 90°$ with a half-cone angle of $\sigma \approx 35°$. Magnetic fields 0, 0.1630, 0.3130, 0.4930, 0.7730,1.0950, 1.4200, 1.8840, 3.2590, and 5.0000 T.

The effect of this anisotropy can be illustrated by plotting the contribution to the total MCD intensity of a purely *xy*-polarized transition of molecules with *z*-axes lying at an angle of ϑ to the applied field (Figure 6). In the case of an isotropic molecular distribution, the maximum intensity arises from molecules lying at an angle of $\vartheta = 45°$. The overall shape of the plot arises because the MCD intensity of an *xy*-polarized transition varies from a maximum at $\vartheta = 0°$ to zero when $\vartheta = 90°$, whereas the number of molecules lying at ϑ increases from $\vartheta = 0°$ to a maximum at $\vartheta = 90°$. At low magnetic fields, the maximum value is displaced from 45° because of the influence of the anisotropy of the zero-field splitting. The distribution of intensity as a function of increasing magnetic field is shown in Figure 6. The total MCD intensity detected at a given wavelength is obtained by integration of the curve. The distribution of MCD intensity in the case of $\vartheta_0 = 90$ and $\sigma = 40°$ is also plotted in Figure 6B. The maximum of the MCD intensity shifts to ~65°, and the integrated MCD intensity decreases to ~30% of its value for randomly oriented samples.

Figure 7 shows the magnetization curves calculated for an *xy*-polarized transition with various distributions of $Mn_{12}C_{15}$ clusters compared with molecules randomly distributed in frozen solution. The solid line represents the curve for an isotropic solution; the dotted line, showing a steeper initial slope, arises for molecules oriented preferentially with the unique axis normal to the film plane, $\vartheta_0 = 0°$; while the dashed line is for molecular axes oriented in the film plane, $\vartheta_0 = 90°$, with a spread of angles, $\sigma = 45°$, in both cases. In every case, at fields of $H >$ 2 T, the saturation behavior of the magnetization curves is similar. By inclusion of a distribution anisotropy into eq 3, the magnetization curves (Figure 4B) can be satisfactorily fitted with a value of $\vartheta_0 = 90°$ and an angular spread of $\sigma \approx 35°$, regardless of the polarization of the transition. Calculations further show that, in the case of an anisotropic distribution with the above spread, the MCD absolute intensity will decrease only about ~30% compared to the intensity of the MCD bands in isotropic solution. The intensity ratios of the MCD bands within a

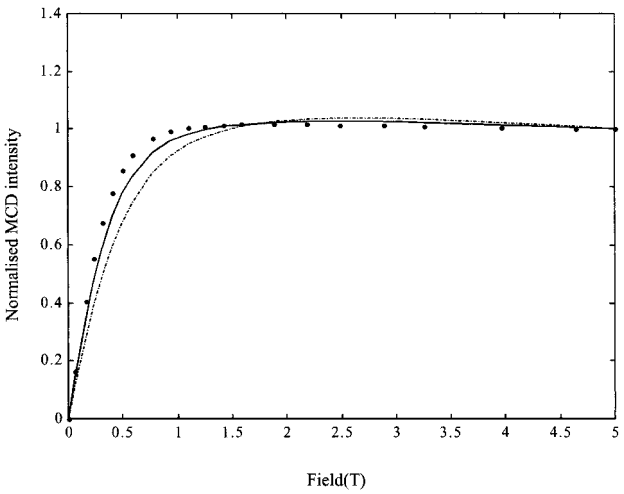

Figure 7. Calculated MCD magnetization for an *xy*-polarized transition from a ground state with $S = 10$, $D = -0.6$ K at 4.2 K with randomly distributed (—) and anisotropically distributed molecules with *z*-axis in-plane, $\vartheta = 90°$ (— · —), and perpendicular to the plane, $\vartheta = 0°$ (···).

Table 1. Linear Polarizations of Transitions of $Mn_{12}C_{15}$ in PMM Film Calculated from MCD Magnetization Curves, Allowing for Partial Orientation

transition energy, $\times 10^3$ cm^{-1}	linear polarization of transition (%)	
	xz/*yz*	xy
28.0	48	52
26.0	45	55
23.5	6	94
21.2	43	57
19.6	9	91
18.0	25	75
15.5	62	38
13.5	14	86

spectrum are relatively insensitive to such a nonuniform distribution, since contributions to magnetization curves from *B* terms do not exceed 20%. Therefore, we conclude that, in PMM polymer films, the $Mn_{12}C_{15}$ clusters tend to orient their easy axes in the plane of the film.

It was unexpected that partial orientation would be generated in PMM films of $Mn_{12}C_{15}$. The films are cast by solvent evaporation that takes place from a solution poured onto a glass slide. The resulting preferential orientation with the *z*-axis oriented into the plane of the film arises from strain across the thickness of the film caused by higher rates of solvent evaporation from the face of the film compared with that at the edges. $Mn_{12}C_{15}$, with long-chain aliphatic ligands, is disk shaped, the short axis being parallel to *z* and the longer axes to *xy*. Thus, stretching the film by evaporation along the normal to the plane presumably causes partial orientation of the long axes of the disk along the normal.

This analysis allows the determination of the MCD magnetization curves and the determination of the polarization ratios. Table 1 summarizes the polarization ratios obtained for $Mn_{12}C_{15}$ in PMM films. The transitions fall into two broad groups: those at 23 500, 19 600, and 23 500 cm^{-1} are predominantly *xy*-polarized, whereas those at 21 200 and 26 000 cm^{-1} are largely polarized *xz* or *yz*.

MCD Magnetization Properties below the Blocking Temperature. Below the blocking temperature of 3 K, spin relaxation becomes extremely slow, and the magnetic properties depend on the temperature and field history of the sample. Upon cooling either frozen glass or film samples of $Mn_{12}Ac$ and $Mn_{12}C_{15}$ from 4.2 to 1.7 K in a field of 5 T, there is very little change in the intensity of the MCD spectra, showing that no significant redistribution of populations among the sublevels takes place; that is, the samples are fully magnetized at 4.2 K in a field of 5 T, as can be judged from the magnetization curves. At 1.7 K, after reduction of the magnetic field to zero, there remains an intense CD spectrum. The sign of the spectrum depends on the direction of the initial magnetizing field (Figures 2 and 3). Thus, the CD spectrum at 0 T reports the magnetic history of the sample. But the extent of retention of magnetization varies between samples with the wavelength at which it is monitored and also shows some variation with the nature of the medium in which the sample is dissolved. For example, in the film sample of $Mn_{12}C_{15}$, the transition at 21 200 cm^{-1} loses approximately 30% of its signal on decreasing the field from 5 to 0 T, whereas the peak at 19 600 cm^{-1} is virtually unchanged. The *xy*-polarized transitions at 19 600 cm^{-1} retains almost 100%, whereas the transition at 21 200 cm^{-1}, polarized *xyz*, retains between 68 and 70% of the magnetization at 4.2 K. By contrast, spectra of samples of $Mn_{12}Ac$ in both film and solution at 1.7 K and at fields of 5 and 0 T are shown in Figure 3. The solution sample retains only about 30% of its initial intensity after removal of the field, in agreement with results obtained previously.[10] The film sample, however, retains about 70% intensity at 0 T, significantly more than the frozen solution.

To explore further the origins of these differences, we have measured MCD hysteresis loops, analogous to susceptibility hysteresis loops, by monitoring the MCD intensity at 1.7 K at a fixed wavelength of selected optical transitions. The field was set initially in one direction at +2.5 T so as to be completely polarizing and then decreased in steps of ca. 0.15 T, through zero-field, to −2.5 T in the opposite sense. After each field increment, the MCD intensity became static after a period of ca. 30 s, at which time the intensity was recorded. MCD hysteresis loops are given for a PMM film sample of $Mn_{12}C_{15}$ at 19 600 and 21 200 cm^{-1} (Figure 8A) and for $Mn_{12}Ac$ at ∼21 000 cm^{-1} (Figure 8B) in frozen glass and in PMM film. One parameter of the hysteresis loop is the coercive field, here defined as half the width of the loop at zero MCD intensity. The coercive fields measured by MCD intensity are summarized in Table 2, and compared with those obtained for a single crystal of $Mn_{12}Ac$ with the field aligned along the unique axis.[8] The retention of magnetization and hence the magnitude of the coercive field vary widely. Given that the samples studied by MCD are isotropic or only partially ordered, the coercivity, for example, of $Mn_{12}C_{15}$ in PMM measured via an *xy*-polarized transition is at first sight surprisingly high at 1.24 T or ∼70% of the value for an oriented single crystal with $H||z$.

The wavelength and polarization dependences of the hysteresis loops and coercive fields are seen clearly for $Mn_{12}C_{15}$ in PMM (Figure 8A). For example, at 19 600 cm^{-1} the loop has a coercive field of 1.24 T, whereas that obtained at 21 200 cm^{-1} is ∼1.0 T. The remnant magnetization at zero field is 75% and ∼60%, respectively.

The magnetic properties determined at a single wavelength represent the sum of a subset of molecular orientations with respect to the direction of the field. The MCD intensity at 1.7 K which arises from the lowest Kramers doublet, $M_s = \pm 10$, is

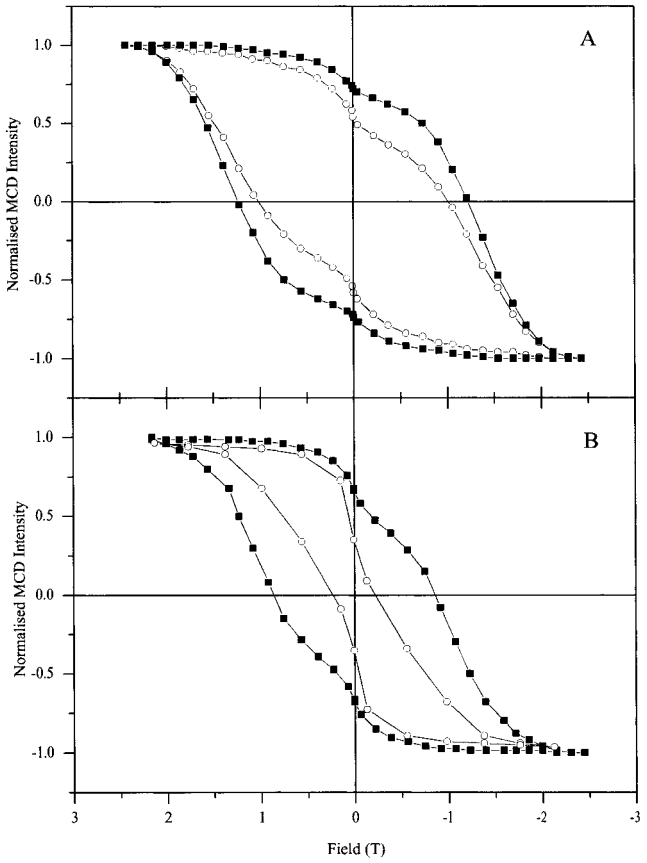

Figure 8. (A) Hysteresis loops of $Mn_{12}C_{15}$ in PMM film measured at 1.7 K and at 21 200 (■) and 19 600 cm^{-1} (○). (B) Hysteresis loops of $Mn_{12}Ac$ measured at 1.7 K at 21 200 cm^{-1} in PMM film (■) and in dmf/MeCN (3:1 v/v) solution (○).

Table 2. Coercive Fields of Mn_{12} Compounds

compd	nature of sample, method of measurement	coercive field at $T = 1.7$ K, T
$Mn_{12}Ac$	single crystal ($H\|\|z$),[a] susceptibility	1.85
$Mn_{12}Ac$	frozen solution (dmf/MeCN)	0.23
	xz,*yz*-polarized transition at 21 200 cm^{-1}, MCD	
$Mn_{12}Ac$	PMM film	0.85
	xz,*yz*-polarized transition at 21 200 cm^{-1}, MCD	
$Mn_{12}C_{15}$	PMM film	1.00
	xz,*yz*-polarized transition at 21 200 cm^{-1}, MCD	
$Mn_{12}C_{15}$	PMM film	1.24
	xy-polarized transition at 19 600 cm^{-1}, MCD	

[a] Reference 4.

given by eq 4. This shows that the temperature-dependent contribution to the MCD intensity arises only from an *xy*-polarized transition, the temperature-dependent term being proportional to $\tanh(g_{\|}\beta H \cos(\vartheta/2kT))$. Because the field is applied parallel to the direction of propagation of the light beam, a single molecule will yield maximum MCD intensity when it is oriented with the *z*-axis parallel to the applied field, $\vartheta = 0°$, and zero MCD intensity at $\vartheta = 90°$. However, the number of molecules lying between ϑ and $\vartheta + \delta\vartheta$ is zero at $\vartheta = 0°$ and a maximum when $\vartheta = 90°$. Thus, in an isotropic medium, the observed MCD intensity is weighted by the contributions from an assembly of molecules between $\vartheta = 0°$ and 90°, with those at $\vartheta = 45°$ making the largest contribution.

For an *xz*- or *yz*-polarized transition, the contribution to the MCD intensity is via the second term in eq 4. It is temperature

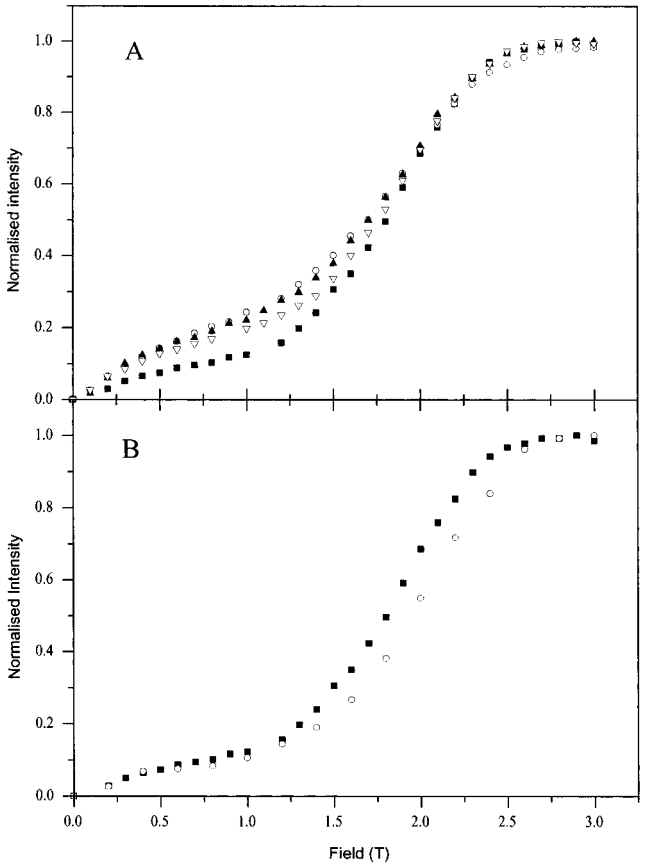

Figure 9. (A) Normalized MCD intensity against applied magnetic field for a selection of transitions of $Mn_{12}C_{15}$ in PMM film. The field was swept to 5 T at 0.004 T s^{-1}, 1.7 K (data to 3 T shown), and the intensity monitored continuously: (○) 18 000, (■) 19 600, (▲) 21 200, and (▽) 23 400 cm^{-1}. (B) Normalized MCD intensity against field for the transition at 19 600 cm^{-1} in $Mn_{12}C_{15}$ in PMM film at 1.7 K and sweep rates of (■) 0.004 and (○) 0.010 T s^{-1}. The field was swept to 5 T (data shown to 3 T) and the intensity monitored continuously.

independent and proportional to *Hg*/*D*. The relative contribution to the loops as a function of the polarization of the optical transition is not the only factor at play. Variation in the relaxation properties of molecules at different orientations is also present because, as ϑ varies, the magnitude of the component of the applied field perpendicular to the unique molecular axis varies. Relaxation can be enhanced by a field component perpendicular to the unique axis. This effect is evident as polarization-dependent responses are observed in magnetization experiments performed at 1.7 K.

The intensities of individual transitions of a zero-field-cooled sample of $Mn_{12}C_{15}$ were monitored at 1.7 K as a function of increasing field between 0 and 3 T. A wavelength-dependent response to changing magnetic field was again observed (Figure 9). The shape of the curves shows a relatively small initial gain of magnetization, followed by a region from 1.5 to 2.5 T of rapid intensity gain until the transition is saturated at ~2.5 T. The transition at 19 600 cm^{-1} shows a lower gain in intensity initially, whereas the transition at 21 000 cm^{-1} shows a greater degree of magnetization at low fields. The magnetization curve of the transition at 19 600 cm^{-1} was obtained at two sweep rates, 0.010 and 0.004 T s^{-1}, at 1.7 K (Figure 9B). The curves overlay up to a field of 1.25 T, but at higher field the curve obtained at 0.010 T s^{-1} has less intensity at a given field than the curve obtained at 0.004 T s^{-1}. This indicates that, at high

field, the relaxation processes responsible for the intensity gain are occurring on a time scale similar to the sweep rates used. At lower field (below 1.25 T), the small, polarization-dependent increases in intensity occur as a function of the changing magnetic field.

It is interesting to note that the shape of the low-temperature magnetization curves is very similar to the $0 \rightarrow (-3)$ T half of the hysteresis loop (Figure 8). During the collection of the magnetization data, it was noticed that, during the sweep to a particular field, the relaxation was fast. However, once the field had been reached, relaxation continued but at a very much slower rate. The similarity of the hysteresis loop to the magnetization curve is perhaps not surprising despite the very different times (hours vs minutes) taken for acquisition of the data. Both measurements are reporting the intensity changes associated with the initial fast phase of relaxation, and the very slow subsequent relaxation makes little impact on the shape of the curves.

The shape of the magnetization curve obtained at 1.7 K, i.e., slow initial magnetization followed by a region of faster magnetization, has been observed by Hernandez et al.[15] at low temperatures on an oriented powder of $Mn_{12}Ac$. The explanation given was that at low fields the energy barrier to interconversion of spin is large and at low temperatures slow relaxation is expected (relaxation time with temperature following the Arrhenius law). As the field is increased, the energy barrier to interconversion of spin polarization is lowered and equilibration of populations becomes rapid. The measurements were performed, and as the field increased, steps similar to those observed in hysteresis measurements were observed (see below). Steps are not observed in the data presented here as a result of a degree of orientation averaging.

The *xz*,*yz*-polarized transition showed the largest initial increase in magnetization, whereas prior to the onset of fast magnetization the transition at 19 600 cm^{-1} (strongly *xy*-polarized) gains only 10% of its saturated intensity. These differences arise from the temperature-independent but linear-field-dependent component. Other studies support this.[13]

Hysteresis loops measured on single-crystal[8] and oriented polycrystalline samples[9] of $[Mn_{12}O_{12}(O_2CR)_{16}\cdot 4H_2O]$ show steps at regular intervals of field. The steps occur at fields where the $M_s = \pm n$ sublevels are isoenergetic, thus allowing QM tunneling through the barrier and increasing the rate of relaxation.[8,9,16] Absence of steps and a low coercive field were observed in a hysteresis loop obtained for a randomly oriented polycrystalline sample of a related $Mn_{12}O_{12}$, $S = 9$ core.[17] The hysteresis loops obtained using MCD spectroscopy in frozen solution and in films exhibit characteristics of both unoriented powder and single-crystal samples, depending on the optical wavelength selected for monitoring the ground-state magnetization. The loops show a single step, at 0 T, and have lower coercive fields than those measured for single-crystal samples.[8] The observation of a step at 0 T only is readily explainable. At zero field, all $n = \pm$ pairs of sublevels are coincident in energy, leading to an increase in relaxation rate via tunneling and hence a step in the hysteresis loop. No further, resolved steps are observed, since within the subset of molecules selected by wavelength there will be a distribution of molecular orientations. This will lead to a "smoothing out" of the steps observed in the oriented single-crystal measurements.

The hysteresis loops obtained for the transition at 21 200 cm^{-1} of $Mn_{12}Ac$ in solution and film are different (Figure 8B), the solution sample showing a coercive field of approximately 0.3 T and a substantially smaller remnant signal at 0 T. The coercive field of a film sample is approximately 0.85 T. These factors suggest that the solution sample has a faster rate of relaxation than the film sample. Christou et al. have crystallized two forms of the cluster $[Mn_{12}O_{12}(O_2CC_6H_4Me\text{-}4)_{16}\cdot 4H_2O]$, one form solvated, the other hydrated.[18] Although the structures are very similar, the out-of-phase ac susceptibility measurements established that the solvated cluster had a significantly faster rate of tunneling of magnetization than the hydrated form. The difference in magnetic behavior between the clusters has been explained by the presence of a misaligned Jahn−Teller axis of one of the outer Mn(III) ions in the solvated form.[18] Wernsdorfer et al.[19] have also identified, by means of differences in relaxation rates, two forms of $Mn_{12}Ac$ in a crystalline sample. The faster relaxing form (present as a minority species) was shown to have an anisotropy barrier of 45 K, approximately 20 K lower than the barrier of the majority $Mn_{12}Ac$ species. The MCD spectrum of the $Mn_{12}Ac$ in solution indicates that there is some distortion at the Mn(III) ions. This, coupled with the altered magnetic properties of the $Mn_{12}Ac$ cluster in solution, supports the above findings that solvent and solvent of crystallization can have a considerable influence on relaxation rates observed. The results show that the optical and magnetic properties of $Mn_{12}Ac$ are perturbed in a solution of MeCN/dmf, possibly because dmf is a strongly coordinating O-donor solvent.

Conclusions

To allow optical studies of the magnetic properties of single-molecule magnets based on the core mixed-valence framework, $Mn_{12}O_{12}L_{16}$, we have exchanged the acetate ligands, L, for long-chain carboxylic acid, $C_{14}H_{29}COOH$, that confers better solubility in organic solvents. This has enabled thin polymer films of these compounds in poly(methyl methacrylate) to be cast by solvent evaporation, providing samples suitable for variable-temperature and variable-field MCD studies. The film is very durable with respect to cycling to ultralow temperature, and the polymer does not absorb at wavelengths longer than ca. 300 nm. Although the absorption spectra in isotropic light are broad, steadily increasing toward the UV, the low-temperature MCD spectra contain resolved features both positive and negative. By measuring MCD magnetization curves at various optical wavelengths at 4.2 K between 0 and 5 T, we have determined the polarizations of the optical transitions relative to the unique axis of the zero-field distortion. The MCD magnetization curves measured at 4.2 K between 0 and 5 T for the case of $Mn_{12}C_{15}$ in the PMM film can be fitted only on the assumption of

(15) Hernández, J. M.; Zhang, X. X.; Luis, F.; Bartolomé, J.; Tejada, J.; Ziolo, R. *Europhys. Lett.* **1996**, *35*, 301−306.
(16) (a) Friedman, J. R.; Sarachik, M. P.; Hernández, J. M.; Zhang, X. X.; Tejada, J.; Molins, E.; Ziolo, R. *J. Appl. Phys.* **1997**, *81*, 3978−3980. (b) Luis, F.; Bartolomé, J.; Fernández, J. F.; Tejada, J.; Hernández, J. M.; Zhang, X. X.; Ziolo, R. *Phys. Rev. B* **1997**, *55*, 11448−11456.
(17) (a) Barbara, B.; Thomas, L.; Lionti, F.; Sulpice, A.; Caneschi, A. *J. Magn. Magn. Mater.* **1998**, *177*−*181*, 1324−1329. (b) Lionti, F.; Thomas, L.; Ballou, R.; Barbara, B.; Sulpice, A.; Sessoli, R.; Gatteschi, D. *J. Appl. Phys.* **1997**, *81*, 4608−4610.
(18) Sun, Z.; Ruiz, D.; Dilley, N. R.; Soler, M.; Ribas, J.; Folting, K.; Maple, M. B.; Christou, G.; Hendrickson D. N. *Chem. Commun.* **1999**, 1973−1974.
(19) Wernsdorfer, W.; Sessoli, R.; Gatteschi, D. *Europhys. Lett.* **1999**, *47*, 254−259.

nonrandom distribution of molecular *z*-axes. The variation of the MCD intensity versus temperature at relatively low magnetic fields shows changing spin population across the manifold of zero-field split levels of the $S = 10$ ground state and has established the axial ZFS parameter D at -0.61 K, very similar to that determined for single crystals of $Mn_{12}Ac$. The MCD-detected hysteresis curves have been measured in frozen solution and in PMM films at 1.7 K, below the blocking temperature. The retention of spin polarization, after reduction of a polarizing magnetic field to zero, in films can be surprisingly high when detected with the population selectivity of zero-field CD. For a single crystal of $Mn_{12}Ac$ with the applied magnetic field parallel to the axis of axial distortion, the coercive field is 1.85 T. In a sample in which the $Mn_{12}O_{12}$ cores are randomly oriented, the retention of magnetization can be up to 70% of this value. The utility of the technique of MCD spectroscopy in the study of molecular magnets, providing an optical readout of the state of the spin polarization, has been demonstrated. By taking advantage of the polarization of the optical transition, a subset of molecular orientations with respect to the direction of field is selected. Individual transitions represent different orientational subsets. Thus, from randomly or partially oriented samples, orientation-dependent properties can be probed directly with high sensitivity.

Acknowledgment. The authors thank the EPSRC (GR/M14395/01) and BBSRC for support of this work.

JA020456B